

# Fabri-perot scanning probe for near-field optical microscopy

Yu.N. Kulchin<sup>1</sup>, O.B. Vitrik<sup>1</sup> and A.A. Kuchmizhak<sup>1,#</sup>

<sup>1</sup> Institute for Automation and Control Processes of Far Eastern Branch of Russian Academy of Science (IACP FEB RAS) Radio St., 5, Vladivostok, Russia  
# Corresponding Author / E-mail: ku4mijak@mail.dvo.ru, TEL: +7-914-070-1626, FAX: + 42-3231-0452

KEYWORDS : near-field optical microscopy, aperture-based probe, fiber optic Fabry-Perot interferometer, FDTD method

*We have developed a new approach in scanning near-field aperture-based optical microscopy consist in transition from amplitude registration of light radiation intensity to the interferometric detection of small phase changes inside the scanning probe based on the fiber optic Fabry-Perot interferometer with subwavelength aperture formed in one of its output mirrors. When scanning a test object with such a probe, the resonant frequency of the interferometer undergoes modulation owing to the interaction of the evanescent light field formed by the aperture with the test sample. Using the information about the value of the resonant frequency shift one can recover the surface topography with high spatial resolution. Laboratory prototype of the scanning interferometric probe showed the spatial resolution of  $\lambda/14$ . The numerical analysis indicates the possibility of further increases in the proposed resolution microscopy to  $\lambda/40$ .*

Manuscript received: January XX, 2011 / Accepted: January XX, 2011

## NOMENCLATURE

$\lambda$  = wavelength of the laser source in use  
D = output aperture diameter  
h = distance between the scanning probe aperture and the test sample  
L = length of the fiber optic resonator

## 1. Introduction

Investigation of topographical peculiarities of nanostructured objects with high spatial resolution was always important when conducting a wide range of investigations in micro- and nanoelectronics, microbiology, etc. Nowadays scanning near-field optical microscopy (SNOM) [1,2] is one of the most prospective and effective techniques of investigation of objects with sizes that are impossible to be defined with the help of classical optics methods because of fundamental diffraction limit action. Though the current worked out SNFOM systems are inferior to the methods of scanning probe microscopy that use nonradiating fields (atomic-force or tunnel electron microscopy) in resolvability, however they do not demand vacuum for work process and give the possibility to get optical

images of nano-sized objects with subwavelength spatial resolution [3]. Also these systems yield to conduct fundamental investigations in local spectroscopy of microbiological [4,5] and semi-conducting objects (quantum dots, wells, threads, etc.) [6,7] and to carry out modifications of surface structures for superdense information record with spatial resolution less than 100 nm [8-10].

The basis of the most common modification of SNOM methods is provided by a principle of photodetector registration of light radiation intensity; the radiation is formed by a scanning aperture probe and diffracted by microroughnesses of the test sample [3]. Usually, the probe is made in the form of vastly tapered optical waveguide with a quantum optical core covered with metallic covering. In this case it is possible to overcome diffraction limit of optical systems due to localization of partial power of the light radiation about the subwavelength exit aperture of the probe by way of so-called evanescent (nonradiating) field. As a rule, the probe exit aperture diameter which defines resolvability of the SNOM systems is not made less than  $\lambda/10$ , where  $\lambda$  – wave-length of the radiation in use. Otherwise, light power attenuation at the below-cutoff part of waveguide is extremely large and sensitivity of the photodetectors is not enough to register small variations of the radiation intensity diffracted on microroughnesses of planar relief [11]. Thus, poor sensitivity of the registration method in use applies restriction on size of the probe exit aperture and correspondently on spatial resolution of

the aperture SNOM systems.

Usage in measuring systems the interferential-based principles of registration instead of amplitude ones is known to lead to the significant increase of sensitivity [12]. That is why it is appropriate to increase sensitivity and, as a consequence, resolvability of the aperture methods of scanning near-field optical microscopy due to registration of phase changes of the radiation directed along the probe. These changes are caused by interaction of the evanescent field formed by this radiation with the test sample. One of the most sensitive types of interferometers which are able to register extremely small phase changes of optical radiation is a Fabry-Perot interferometer. As a result, the goal of this paper is investigation of possibility to use the aperture probe on basis of the fiber optic Fabry-Perot interferometer in the SNOM systems.

## 2. Numerical Simulation of the fiber optic Fabry-Perot scanning probe

This paper reviews a probe in form of the fiber optic Fabry-Perot interferometer schematically viewed in figure 1. Its resonator ( $L$ ) is made by a segment of cylindrical two-layer optical fiber (OF) with step-index profile. The end surfaces of the segment are covered with mirror coverings (2, 3). In one of the mirrors there is a nano-sized diaphragm (4) as a subwavelength light source of the radiation. When using the probe scheme like this it is supposed that the phase changes of the radiation in the interferometer resonator that are caused by interaction of the localized light field on exit from the nano-sized diaphragm with the test sample (5) must lead to a shift of resonant modes in the Fabry-Perot interferometer. According to the value of this resonant frequency shift it is possible to define the distance between the diaphragm and the test sample.

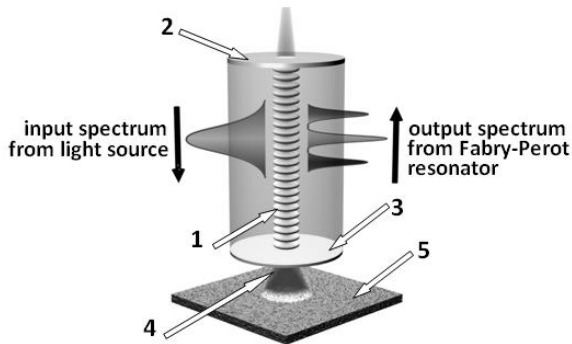


Fig. 1. Schematic layout of the fiber optic Fabry-Perot interferometer under investigation

This supposition was tested in this paper with the help of a finite-difference time-domain method (FDTD) to solve Maxwell's equations [13]. This method has already shown its effectiveness when calculating parameters of electromagnetic field in optical media with subwavelength inhomogeneous including aperture-based [14] and apertureless probes [15].

When making calculations it is supposed that the optical fiber segment used to form the probe has an optical core with refractive index  $n_1=1.473$ , diameter  $d_{\text{core}}=8 \mu\text{m}$ , and endless covering with refractive index  $n_2=1.469$ . Such a model highly describes optical characteristics of a standard weakly-guiding OF [16]. Precision of refractive indexes of the core and OF covering yields to regard within the bounds of this model a transversal component of electric field  $E_z$  of an electromagnetic wave and its derivative  $\delta E_z/\delta z$  as permanent at

the boundary separating these media [16]. The central length of the wave of the broadband light source ( $\lambda$ ) is  $1,55 \mu\text{m}$ , full-width-at-half-maximum is  $\Delta\lambda = 0,05 \mu\text{m}$ , that assumes stimulation of the only transversal waveguide mode in the OF. The test sample with smooth surface is considered to be ideal electric conductors; according to this, the electric field component  $E_z$  is zero at the boundary with them. Input and output Pt mirrors have frequently dependent permittivity from experimental data [17].

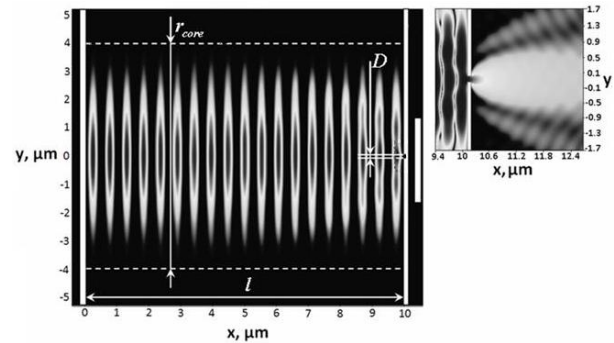


Fig. 2. Distribution of the electric field component  $E_z$  in the parallel-plate fiber optic Fabry-Perot interferometer with the nanosized aperture and in the output of the aperture (inset).

Picture 1 shows the results of numerical calculations of stationary distribution of the electric field component  $E_z$  in the probe-sample system. These results were produced when using the diameter of the diaphragm  $D=\lambda/3$ , length of the resonator  $L=10\lambda$  and the distance between the probe and the test sample  $h=2,6\lambda$ . It is seen that the radiation penetrates through the exit mirror in the area of the subwavelength diaphragm that promotes interaction of the radiation with the test sample. It leads to the shift of the interferometer resonance wavelengths in comparison with a case  $h=0$ . In our test sample this shift is  $\delta\lambda=0,45\cdot 10^{-3}\lambda$ . Picture 2 shows a set of curves demonstrating the calculation results of  $\varepsilon=\delta\lambda/\lambda$  relative to the shift of the interferometer resonance wavelength. These results were produced for different sizes of resonators and diaphragms.

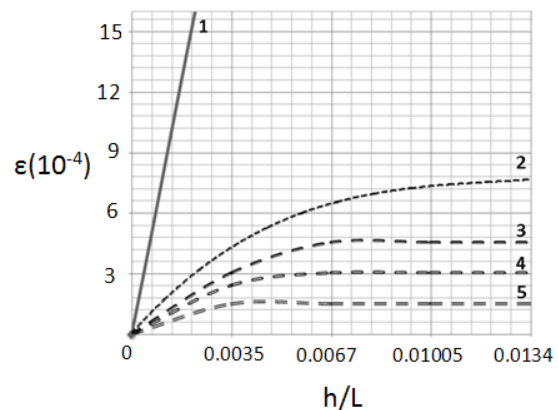


Fig.3. Calculated dependencies of the relative shift of the resonant wavelength  $\Delta\lambda/\lambda$  on the relative displacement  $h/L$  of the test object with the aperture diameter of  $D=5\lambda$  (1),  $\lambda/4$  (2),  $\lambda/8$  (3),  $\lambda/15$  (4) and  $\lambda/40$ (5).

It is seen that the shift of the interferometer resonance wavelength is defined by the ratio  $h/L$ . At the same time, in case of big diaphragms with diameters like diameters of the OF cores the dependence  $\varepsilon(h/L)$  is line (curve 1). Such behavior of the curve can be

explained by the following: the diaphragm with big diameter does not practically influence on spatial distribution of modes in the resonator that are concentrated in its core. In this case the resonator will be formed by the entrance mirror of the interferometer (2, picture 1) and the test sample (5, picture 1); at the same time, change of the sample location just leads to change of length of the resonator like this. Such a model yields to make the simplest analytical calculation [6] showing that  $\varepsilon = \frac{h}{n_1 L}$  that completely coincides with the results produced by the numerical method.

When decreasing the diameter of the diaphragm to subwavelength sizes the direct ratio between  $\varepsilon$  and  $h/L$  is held only for small distances  $h$  comparable with size of the diaphragm (curves 2 – 5, picture 2) due to transformation of the evanescent modes to radiation ones. When increasing  $h$  in future the steepness of the dependence  $\varepsilon(h/L)$  constantly decreases and becomes zero with  $h \gg D$ , when the test sample is out of the coverage of subwavelength source of the radiation.

The steepness of the line part  $\alpha = \frac{L \cdot n_1}{\lambda} \cdot \frac{\delta \lambda}{h}$  of the dependence  $\varepsilon(h/L)$  defining sensitivity of the probe to lengthwise movement of the sample in the coverage of subwavelength source changes from 0,7, (in case, when the diameter of the diaphragm is big) (curve 1) to 0,07 (in case  $D = \lambda/15$ ) (curve 5).

Usage of such mirrors in the Fabry-Perot interferometer supposes forming in it extremely contrasting picture of interference maximums; at the same time the diaphragm with diameter  $D \ll \lambda$  in one of such mirrors does not contribute to broadening of these peaks as it was confirmed by the results of the numerical calculations. In these conditions it is possible to register any extremely small shift of resonance wavelength. However, real mirrors have  $r < 100\%$  that according to the Rayleigh criterion [6] limits the minimum acceptable shift of resonance maximum  $\delta \lambda_{\min}$  of the Fabry-Perot interferometer. Hence, it is easy to show that lengthwise resolution of the suggested method will be defined by  $h_{\min} = L n_1 \frac{\lambda}{\alpha Q}$ , where

$Q = 2\pi L n_1 \frac{\sqrt{r}}{1-r}$  - Q-factor of the resonator failing absorption

loss in it. As appears from the above, the diameter of the probe sensitivity diaphragm  $D = \lambda/15$  is quite enough to yield the lengthwise resolution of order of subwavelength aperture size, if reflection factors of the resonator mirrors will exceed  $r = 93\%$ . It is easy to produce such a reflection factor experimentally even using thin-film metallic mirrors.

### 3. Experimental investigation

To verify results obtained numerically the optical near-field probe based on the fiber optic Fabry-Perot resonator was developed. The probe is formed by the section of the two-layer optical fiber ( $r_{\text{core}} = 9 \mu\text{m}$ ,  $n_2 = 1.4677$ ,  $n_1 = 1.473$ ), which end surfaces was covered by optically thick metal coatings by using ion sputtering method. The thickness of sputtered coatings  $d$  was chosen according to a maximum value of Q-factor required. It was provided by increasing of reflection coefficients of the mirrors  $R$  and, as a consequence, the growth of the thickness of reflective coatings. The greatest coating thickness is required in the case of the output resonator mirror to avoid possible penetration of radiation through the coating outside the

area of the subwavelength aperture, which in turn could lead to misinterpretation of resonant peak shifts. However, the excessive increase of the coating thickness can lead to power losses growth in the cavity and, consequently, to the sensitivity restriction. As a compromise solution, the coating with the thickness of about 45 nm ( $R_1 = 80\%$ ) was formed on the input end surface of the optical fiber. On the output surface the coating with a little more thickness ( $\sim 80$  nm,  $R_2 = 98\%$ ) was made. As it was shown in experiments, this solution provides the value of Q-factor of about  $0,5 \cdot 10^5$ , and also eliminates feasible interaction of radiation with the test sample outside the area of the subwavelength aperture.

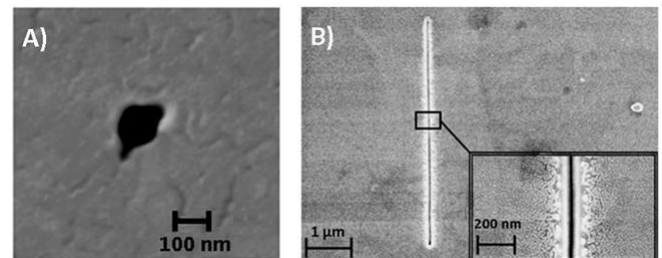


Fig.4. Electron scanning images of the apertures fabricated with use of FIB method: circular aperture with  $D = \lambda/15$  (A) and slit aperture with the width  $w = \lambda/40$  and length  $r = 5 \mu\text{m}$  (B)

Subwavelength aperture with different shapes (Fig. 4) in the output resonator mirrors was made by ion-beam etching (Carl Zeiss CrossBeam 1540-ESB). Shape of the diaphragm in Figure 4, approximates to circular shape of the output diaphragm of the standard aperture probe. Potentially it provides the same spatial resolution along each coordinate axis, comparable to the diameter of the hole. However, as it seen from the electron image presented owing to technological difficulties we couldn't achieve the ideal circular form. The slit aperture (fig.4, b) seems optimal for scanning along one of the sample axes, i.e. object with the central symmetry. In addition, this shape corresponds better to the numerical model considered in this paper because it proposes infinite length of the aperture along one of axes.

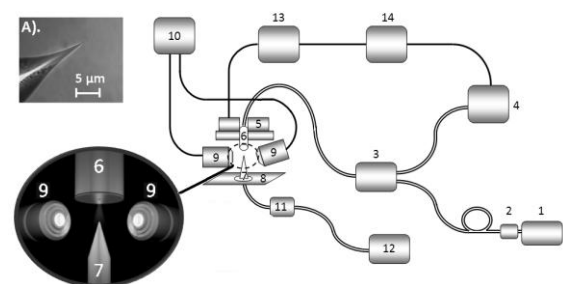


Fig.5. A schematic layout of the experimental set-up: 1-laser source, 2-polarizer, 3-2x1 optical coupler, 4-optical spectrum analyzer, 5-scanning system, 6-scanning FP probe, 7-test object, 8-scanning system, 9-microscope objectives, 10-image processing system, 11-photodetector, 12-digital oscilloscope, 13-position control system, 14-PC. Inset A: optical image of the apex of the test object in use.

For experimental investigations of the dependence of the resonant maximum shifts on the displacement between the subwavelength aperture and the test sample the experimental setup depicted on the

figure 5 is used. Due to technological problems it is difficult to achieve very small apertures ( $D < 100$  nm), so the broadband semiconductor diode was used as a light source with the sufficiently high central wavelength  $\lambda_c = 1553$  nm. It allowed us to achieve the relationship between the wavelength utilized and the diameter of the aperture  $\lambda/D \sim 15$ . The test sample was chosen according to following reasons. On the one hand, the test sample must have the size, which exceeds the diameter of the subwavelength aperture. It provides the maximum efficiency during the interaction of sample with light field localized in the vicinity of the aperture. On the other hand, to simplify the process of positioning the sample tip near the aperture, the size of the latter should be much smaller than the diameter of the output mirror of the resonator. Therefore the tapered optical fiber with the apex radius of curvature  $\sim 300$  nm is used as a test sample. Positioning and scanning of the test object near the aperture is performed by the scanning system, which provides the scanning accuracy  $\sim 10$  nm. In the case of the slit aperture the polarization direction is maintained perpendicular to the slit exactly as it was considered in the numerical model.

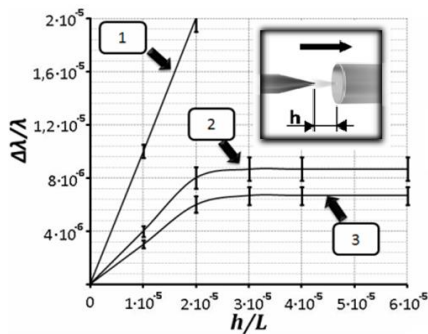


Fig.6. The dependence of the relative shift of the resonant wavelength  $\Delta\lambda/\lambda$  on the relative displacement  $h/L$  of the test object: curve 1 was obtained for case of the aperture diameter  $D=5\lambda$ , curve 2 – circular aperture  $D=\lambda/15$ , curve 3 – slit aperture with the width  $w=\lambda/40$ ;

Investigation results of the dependence of the relative shift of the resonant maxima on the relative displacement between the subwavelength aperture and the test sample  $\delta\lambda/\lambda(h/L)$  for cases of the circular aperture (curve 2) and the slit (curve 3) are presented in figure 6. As it seen from the data presented, the character of the experimental curves corresponds to numerical ones: linearity is held only for small distances  $h$  comparable with size of the diaphragm and when increasing  $h$  the steepness of the dependence  $\delta\lambda/\lambda(h/L)$  gradually decreases and becomes zero with  $h \gg D$ , when the test sample is out of the coverage of subwavelength source of the radiation.

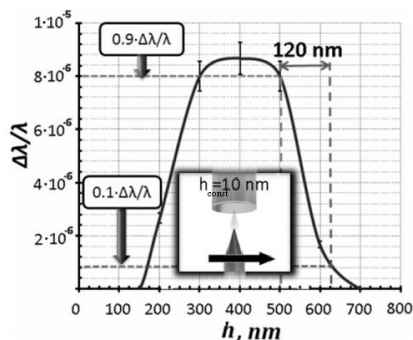


Fig.7. Scanning of the apex of the test object by the Fabry-Perot probe with the circular aperture along the Y-axis in constant-height mode.

The results of scanning the tip of the sample by the resonator with the circular aperture along the y-axis in the constant height mode (the distance  $h$  between the tip and the aperture  $\sim 20$  nm) are presented in the figure 7. According to the data presented, the value of the lateral resolution, defining as the transition from 10% to 90% of the signal levels difference, reaches  $\sim \lambda/15$ .

Thus possibility of creating a new type of interferometric aperture-based probe for near-field optical microscopy based on a fiber optic Fabry-Perot resonator with the nanosized aperture is investigated theoretically and experimentally. The method developed allows one to achieve the values of longitudinal and lateral resolutions not worse than 120 nm, which corresponds to  $\lambda/15$  for wavelength of the source  $\lambda=1550$  nm.

## ACKNOWLEDGEMENT

Authors gratefully thank for AFM and SEM investigations and assistance A.A. Nepomniashiy. Special thanks to go to E.V. Pustovalov of Far Eastern Federal University for making apertures using FIB.

## REFERENCES

1. Betzig E., Trautman J.K. et al., Science. Vol. 251, pp.1468, 1991.
2. Pohl D.W., Denk W., Lanz M. Appl. Phys. Lett. Vol. 44, pp. 651–653, 1984.
3. Hecht B., Sick B., Wild U. P. et al., J. Chem. Phys., Vol. 112, pp. 7761-7774, 2000.
4. Mannelquist A. Iwamoto H. et al. Appl. Phys. Lett, Vol.78, № 14, 2001.
5. Weiss S., Science, Vol. 283, p.1676, 1999.
6. Leen J.B., Hansen P., Cheng Y., Gibby A., Hesselink L. Appl. Phys. Lett. Vol. 97, p. 073111, 2010.
7. Sendur K., Peng C. and Challener W., Phys. Rev. Lett., Vol. 94, pp. 043901, 2005.
8. Nagahara L.A., Yanagi H., Tokumoto H., Nanotechnology, Vol. 50, № 8, 1997.
9. Matsuda K., Saiki T., Saito H., Nishi K. Appl. Phys. Lett, Vol.76, № 73, 2000.
10. Davis C.C., Atia W.A., Gungor A., Mazzoni D.L., Pilevar S. Laser Phys, Vol. 11, pp. 243, 1997.
11. Novotny. L. & Pohl. D.W. NATO Adv. Stud. Inst., E184, pp. 21–33, 1995.
12. Born M., Wolf E. "Principles of Optics", Oxford: Pergamon Press, 1969.
13. Taflove A., Hagness S. C. "Computational Electrodynamics: The Finite-Difference Time-Domain Method", Artech House, inc. 2000.
14. Krug, J. T. I., Sanchez, E. J. & Xie, X. S. J. Chem. Phys. Vol. 116, pp. 10 895–10 901, 2002.
15. Malcolm N.P., Heltzel A.J., et al., Appl. Phys. Lett. Vol. 93, p. 193101, 2008.
16. Snyder A., Love J. "Optical Waveguide Theory", Moscow: Radio i Svyaz', 1987.
17. Johnson P.B. and Christy R.W. Phys. Rev. B, Vol.6, pp. 4370, 1972.